HYDRODYNAMIC INTERACTION BETWEEN SHIPS AND RESTRICTED WATERWAYS

E Lataire and **M Vantorre**, Ghent University, Belgium

SUMMARY

In open and unrestricted waters the water displaced by a forward sailing vessel can travel without major obstruction underneath and along the ship. In restricted and shallow sailing conditions, the displaced water is squeezed between the hull and the bottom and/or the bank. This results in higher flow velocities and as a consequence a pressure drop around the same hull. In the vicinity of a bank this pressure drop generates a combination of forces and moments on the vessel, known as bank effects. The major achievement of the presented research is the development of a realistic and robust formulation for these bank effects. This knowledge is acquired with an extensive literature study on one hand and with dedicated model tests carried out in different towing tanks on the other. The majority of the utilised model tests were carried out in the shallow water towing tank at Flanders Hydraulics Research in Antwerp, Belgium. The data set on bank effects consists of more than 8 000 unique model test setups (which is by far the most elaborate research ever carried out on this subject). These model tests provide the input for the analysis of bank effects and the creation of the mathematical model.

Overall the magnitude of the bank induced forces increase with:
- A higher forward speed of the ship
- A higher propeller load
- A lower under keel clearance
- A more confined navigation area: steeper banks, smaller channel width
- A smaller distance between ship and bank

The mathematical model copes with a wide range of ship types and bank configurations and is suitable for implementation (and has been implemented) in full mission bridge simulators which can be used for training purposes as well as for research to support the admittance policy or exploitation of ports and waterways.

NOMENCLATURE

Symbol	Unit	Description
A_M	[m]	midship area
B	[m]	breadth of the ship
C_B	[ ]	block coefficient
d2b	[ ]	dimensionless distance to bank
D	[m]	propeller diameter
Fr_{crit}	[ ]	critical speed
Fr_h	[ ]	Froude number (water depth dependant)
g	[m/s]	gravity constant of the Earth
h	[m]	water depth
L_{pp}	[m]	length between perpendiculars
m	[ ]	blockage ratio
m_{eq}	[ ]	equivalent blockage ratio
N_{BANK}	[Nm]	bank induced yaw moment
T	[m]	draft
T_M	[m]	draft at midship
T_P	[N]	thrust of the propeller
Tu	[ ]	Tuck number
Tu_m	[ ]	Tuck number taking into account blockage ratio
V	[m/s]	forward speed (of the ship)
V_{eq}	[m/s]	equivalent forward speed
V_T	[m/s]	the axial speed in the flow field behind the propeller induced by the propeller
W_h	[m]	width of the canal section at the bottom (or at water depth h)
W_0	[m]	width of the canal section at the free surface
w	[ ]	weight factor
X_{BANK}	[N]	bank induced longitudinal force
x	[m]	longitudinal position (from the midship)
Y_{BANK}	[Nm]	bank induced sway force (overall)
Y_A	[Nm]	bank induced sway force at the aft perpendicular
Y_F	[Nm]	bank induced sway force at the forward perpendicular
y	[m]	lateral position
y_{infl}	[m]	influence width
z	[m]	vertical position
z_h	[m]	height of the submerged platform
Δ	[N]	displacement force
β	[°]	drift angle
δ	[°]	amount of rudder
λ	[ ]	scale factor
ξ_-	[ ]	coefficient of the mathematical model
ρ	[kg/m]	density of the fluid
χ	[ ]	the 'weight' of a cross section
χ_{ocean}	[ ]	the 'weight' of an infinite large cross section
χ_p	[ ]	the 'weight' of the port side cross section
χ_s	[ ]	the 'weight' of the starboard side cross section
χ_{ship}	[ ]	the 'weight' of the ship section
Ω	[m]	canal cross section area

ABBREVIATIONS

CEMT   Conférence Européenne des Ministres de Transport
CFD   Computational Fluid Dynamics
FHR   Flanders Hydraulics Research
PIANC   The World Association of Waterborne Transport Infrastructure
RoRo   Roll on roll off
TEU   Twenty feet Equivalent Unit

1.   INTRODUCTION

Transport of goods over water, one of the oldest modes of transport for mankind, is very cost effective, especially for carrying large amounts of cargo over large distances. To reach her berthing location, a ship has to sail from unrestricted (ocean, sea) to restricted navigation areas (channels, canals, rivers, port areas). The main dimensions of ship sizes have increased dramatically over the last years. For example, the largest capacity container carrier of 2015, the MSC Oscar (19 224 TEU), offers room to more than double the amount of containers the largest container ship of 2003, OOCL Shenzhen (8 063 TEU) can carry. Similar tendencies can be observed for LNG-carriers, bulk carriers and even inland vessels. However, the overall dimensions of natural rivers, manmade canals nor harbours have increased at the same rate. This may result in an increased risk because due to their increased overall dimensions, ships sail closer to the boundaries of the navigation areas and to each other. Such a decrease of the margins could be justified by the spectacular development of positioning systems and their accuracy and reliability. However, it should be borne in mind that the hydrodynamic forces acting on ships due to their motion through the water increase with decreasing distance to the boundaries of the waterway. The resistance of the vessel, for example, will be larger in shallow water than in deeper water for the same vessel at the same forward speed. As the increased hydrodynamic forces have to be overcome by the ship's own means of control, a decrease of controllability will be the result. Efforts to reduce the installed power of ships for environmental reasons (Papanikolaou et al. 2015) will even amplify this evolution.

For determining the conditions of safe navigation, waterway authorities often make use of ship manoeuvring simulators (Figure 1). Simulator studies have proved to be an important tool for developing (and justifying) a safe admittance policy. The same simulators can also be used for training of "navigators" (pilots, captains, skippers, helmsmen). Doing so, the specific shallow water skills of the trainees can be increased and experienced navigators can develop an optimized strategy and prepare in an optimal way for future situations (new vessels and/or harbour layouts). New or different types (or sizes) of ships calling existing harbours, canals or rivers can be investigated; necessary adaptations to the port approaches can be assessed and optimized. Both the impact of the environment on the (manoeuvrability of the) ship as well as the impact of the bathymetry on the exploitation of a navigation area can be thoroughly investigated. Simulator studies, however, are only a reliable base for nautical studies and training if the hydrodynamic effects are mathematically modelled in a realistic way. The accuracy of these mathematical models becomes increasingly important with decreasing margins, which implies that an increased knowledge on ship hydrodynamics in shallow and confined water is required to keep safety of shipping traffic in waterways and harbours to a high level.

Figure 1. Full mission bridge simulator (360+) at Flanders Hydraulics Research, Antwerp, Belgium

2.   BANK EFFECTS

Bank effects are the hydrodynamic (quasi) steady reaction forces on a sailing vessel, caused by the lateral boundaries of the navigation area (viz. banks). The geometry of the banks can be very different, as is illustrated by the variety of banks that can be found in a very limited geographic area (northern Belgium – southern part of The Netherlands). A long section of the canal Ghent-Terneuzen has a sloped bank of about 18° (1/3) at both sides. The sandy bottoms at the Bend of Bath (River Scheldt) and the outer harbour of Zeebrugge are less steep (7° (1/8) and 11° (1/5), respectively). The latter two are not constant sloped up to the free surface but end in a very gentle, almost flat, shallow water area. The steepest banks are, obviously, vertical quay walls which have a main function as a berthing location but also may act as a boundary for a navigation canal (e.g. Deurganck Dock in the port of Antwerp). Locations with similar (and other) bank geometries can be found all over the world.

A new methodology for calculating the ship – bank interaction forces will be proposed, with the aim of covering a broad range of possible bank geometries and ship types (both inland and seagoing vessels). This formulation contains a new parameter for the ship – bank distance, a new blockage ratio and a parameter for the ship's velocity. Finally, this formulation for bank effects is implemented into the mathematical model of a ship

manoeuvring simulator to obtain an accurate and reliable behaviour of ships sailing along any bank.

A displacement vessel, as the name suggests, displaces an (enormous) amount of water, which needs to be removed backwards when a ship is under way. In open and unrestricted waters this water can flow without major obstruction underneath and along the ship's hull. In restricted and shallow sailing conditions, however, the displaced water is squeezed between the hull and bottom and/or bank. This results in higher flow velocities and a pressure drop around the same hull. This pressure drop generates a combination of forces and moments on the vessel.
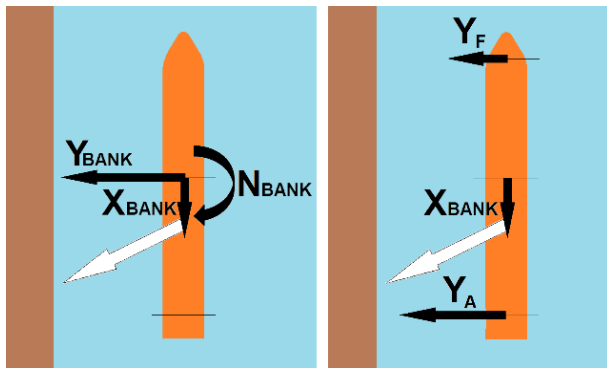
Figure 2. Decomposition of the (horizontal) bank effect (white arrow).

The horizontal bank effects on a ship can be decomposed in three force components (Figure 2), acting in the longitudinal direction (X_{BANK}) and in the lateral direction at the forward (Y_F) and aft perpendicular (Y_A). The latter two lateral forces are in literature mostly presented as the combination of an overall lateral force Y_{BANK} and a yaw moment N_{BANK} (Figure 2). New insight in the phenomenon of bank effects has been acquired with dedicated model tests carried out in different towing tanks (Lataire et al. 2015b).
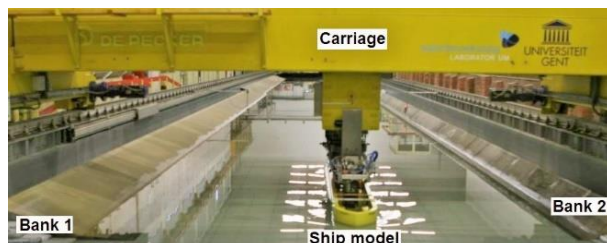

Figure 3. The ship model in the Shallow Water Towing Tank with installed banks.

The majority of the utilised model tests was carried out in the Towing Tank for Manoeuvres in Shallow Water (cooperation Flanders Hydraulics Research – Ghent University) at Flanders Hydraulics Research (FHR) in Antwerp, Belgium (Figure 3). A technical overview of this fully automated towing tank can be found in (Delefortrie et al. 2016).

3. MODEL TESTS

As bank effects are considered to play a major role in the admittance policy for large, deep-drafted ships making use of confined access channels to ports, a research project on the topic was initiated by the administration of the Flemish Government (Belgium). In 2006-2007 thousands of systematic model tests were carried out with two ship models and 8 different bank geometries. In 2010 this systematic series was extended with more than 2,000 model tests with 5 different ship models and 4 surface piercing bank geometries. A limited selection of model tests is made public as benchmark data in (Lataire et al. 2009).

An overview of the ship models which were tested in the frame of the bank effects research project is given in Table 1. For the Belgian ports of Antwerp and Zeebrugge container carriers are responsible for the largest part of their traffic. Therefore two ship models of container carriers have been used. Ship models C0U and C0P represent single screw container carriers with a capacity of 8,000 and 12,000 TEU, respectively, the latter having the maximum main dimensions that can call the new Panama locks. A ship model (G0M) of a 135,000 m LNG-tanker has also been tested along a wide range of bank geometries. The model has been tested at maximum draft only, since this is the more critical situation (smallest under keel clearance and relatively hazardous cargo).

Table 1. Main dimensions ships tested at full scale, values in italic are design drafts

	L_{PP}	B	T_M	Cb	λ
	[m]	[m]	[m]	[ ]	[ ]
A01	190.0	31.0	*7.4*	0.62	50.0
B01	108.0	11.5	*3.7*	0.91	25.0
C0P	348.0	48.8	*15.2*	0.65	80.0
C0U	331.3	42.8	12.0	0.64	80.8
C0U	331.3	42.8	*14.5*	0.66	80.8
C0U	331.3	42.8	13.8	0.62	80.8
G0M	266.6	41.6	*11.0*	0.77	70.0
T0Z	320.0	58.0	*20.8*	0.81	75.0
W01	4.00	0.40	*0.25*	0.44	1.0

The ship model T0Z has the lines of the openly available tanker KVLCC2 (KRISO Very Large Crude Carrier), (Stern & Agdrup 2008) and is of high value for comparing towing tank results worldwide and for validating CFD calculations in deep and shallow water (Zou & Larsson 2013).

Ship model A01, a model of a twin screw Ro-ro ship, has been added to the program for its specific lines and twin screw propulsion system. With respect to bank effects, this

implies that an active propeller is located relatively close to the bank compared to a single screw propulsion system.

Model tests have also been carried out with an inland vessel (B01), the lines of this model are based on the CEMT Class Va. The final model used in present research on bank effects is a so-called Wigley hull (W01). This is not a scaled ship but a mathematically defined geometry (equation 1). A Wigley hull is a popular and easy to mesh hull form for numerical calculations (CFD).

$$|y| = \begin{cases} B \frac{z}{T}\left(2 - \frac{z}{T}\right)\frac{4x}{L}\left(1 - \frac{x}{L}\right) & z < T \\ B \frac{4x}{L}\left(1 - \frac{x}{L}\right) & z \geq T \end{cases} \quad (1)$$

Different banks were installed in the towing tank to investigate the influence of the bank geometry on the forces and moments induced on the vessel. The installed bank did not change in geometry for a significant number of ship lengths because only tests in a steady state regime condition are considered.

Three types of installed banks can be distinguished in present (and other published) research:

- a vertical quay wall **QY**: a surface-piercing vertical wall is positioned in the tank or the walls of the tank itself are used. In Table 2 the slope and canal width at full depth (W_h) is listed.
- A surface piercing wall **SP**: a sloped bank runs at a constant slope from the bottom of the towing tank up to highest water level tested (Table 3). This slope is expressed as the ratio between the rise and run with a normalised rise (Figure 4).
- A semi submerged bank **SS**: a sloped bank starts at the bottom of the towing tank but ends before the free surface is reached. A horizontal (submerged) plane connects the slope with the wall of the towing tank or an installed vertical quay wall (Figure 5 and Table 4).

Table 2. Names and dimensions of the vertical quay walls tested

Name	run/rise	W_h
[]	[]	[m]
QY_0_0.812_0	0	0.812
QY_0_0.966_0	0	0.966
QY_0_1.314_0	0	1.314
QY_0_1.933_0	0	1.933
QY_0_3.865_0	0	3.865
QY_0_4.400_4	0	4.400
QY_0_6.330_0	0	6.330
QY_0_7.00_0	0	7.000

Table 3. Names and dimensions of the sloped banks tested

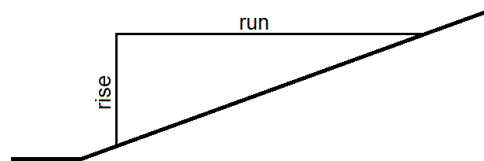| Name	run/rise	W_h
[]	[]	[m]
SP_1_4.200_3	1	4.200
SP_3_4.200_1	3	4.200
SP_3_5.730_0	3	5.730
SP_4_4.400_0	4	4.400
SP_5_4.030_0	5	4.030
SP_8_4.030_0	8	4.030

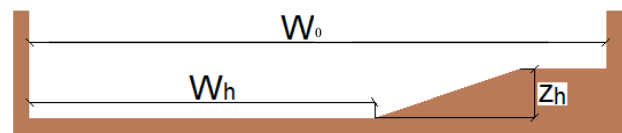Figure 4. Rise and run of a sloped bank

Figure 5. Semi submerged bank properties W_{max}, W_h and z_h

Table 4. Geometric dimensions of the semi submerged banks

Name	run/rise	W_h	z_h	W_0
[]	[m/m]	[m]	[m]	[m]
SS_0_33.00_.245_33.45	0	33.0	0.245	33.45
SS_0_33.00_.305_33.45	0	33.0	0.305	33.45
SS_0_33.00_.305_39.00	0	33.0	0.305	39.00
SS_5_4.030_.120_7.00	5	4.03	0.120	7.000
SS_5_4.030_.150_5.335	5	4.03	0.150	5.335
SS_5_4.030_.150_5.890	5	4.03	0.150	5.890
SS_5_4.030_.150_7.00	5	4.03	0.150	7.000
SS_8_4.030_.150_7.00	8	4.03	0.150	7.000

In Figure 6 all water depth (h) to draft (T) ratios are listed with the number of model tests carried out for each ratio. The water depth is defined as the deepest water depth in the towing tank (independent of the lateral position of the ship). Most of the ship models are tested in 2 to 4 different water depths. In this way, the range of shallow water depths encountered by the vessel is covered.
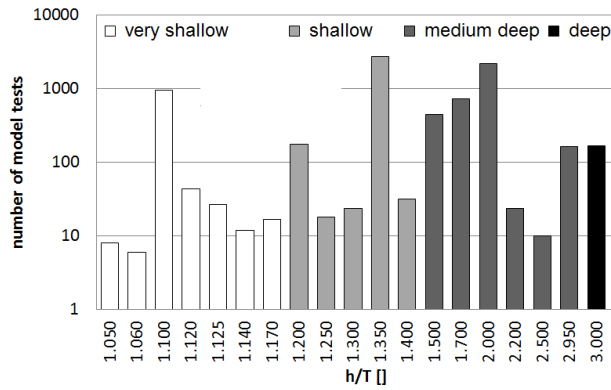
Figure 6. The number of model tests for each h/T ratio

The lateral position of a ship model in a towing tank with banks installed can be defined in different ways. The most straightforward and pragmatic method is by referring to the earth bound coordinate system of the towing tank itself. About five lateral positions are tested for all ship – bank - water depth combinations.

Most ship models are tested at forward speeds of 6, 8 and 10 knots full scale in very shallow water and in shallow water, tests at 12 knots are added and 6 knots excluded. In medium and deep water, forward speeds corresponding to full scale velocities of 14 and 16 knots are added to the test program.

The number of model tests and the corresponding velocities can be plotted to the dimensionless Froude number based on the water depth:

$$Fr_h = \frac{V}{\sqrt{gh}} \qquad (2)$$

With h being the deepest water depth over the entire cross section, as in Figure 6. In case of a sloping bank, the lateral position of the ship model will therefore not change the corresponding Fr_h. Figure 7 displays the distribution of the number of tests over the Fr_h range.
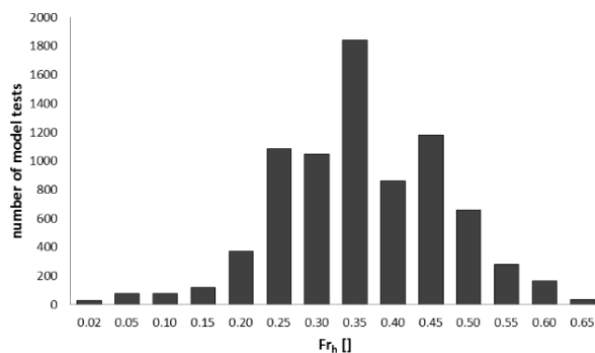

Figure 7. The number of model tests for each Fr_h

The ship models C0U, C0P, G0M, T0Z and B01 are equipped with one propeller while ship model A01 has two propellers. During the test runs, the propeller rate was kept constant at a predefined value between zero and 80% of the harbour full propeller rate for that vessel.

The ship model is forced to follow a predetermined trajectory during captive manoeuvring tests. The ship model is then free to heave and pitch but is rigidly connected to the towing tank mechanism according to the other degrees of freedom. The forces acting on the ship model, the rudder and the propeller are measured as well as the vertical position of the hull, the applied propeller rate and the rudder angle.

4.   BANK GEOMETRY

4.1   DISTANCE TO BANK

In arbitrary cross sections (sloped banks, dredged channels, natural river bottoms with a varying bathymetry) the distance to the banks is ambiguously defined (Figure 8).

Figure 8. A ship in an irregularly shaped cross section

An expression to include the influence of the lateral position in the mathematical model must cope with all the influences exerted by the elements of an arbitrary bank:

- The further away from the vessel the smaller the influence of the geometry.
- No or almost no influence of the bathymetry should be observed at a depth much deeper than multiple times the draft.
- All types of geometries must be covered: sloped banks, semi-submerged banks, changing slope angles, random bank geometries such as natural riverbeds, dredged channels and dredged fairways at sea.

A non-dimensional parameter d2b (distance to bank), based on a weight factor, was introduced (Lataire & Vantorre 2008) to obtain an unambiguous indication for the distance between a ship and a randomly shaped bank. The weight factor w is by definition a value between 0 and 1 which indicates the contribution of a water particle to the bank effects. A water particle closer to the hull will have a value closer to 1 and the weight factor will tend to zero once the water particle is far away from the ship. The closer the water particle is located to the free surface, the larger its weight factor; so, the weight factor decreases with the distance from the vessel and the depth under water. At the cross section of the centre line of the ship and the free surface (at rest) the weight factor is 1.

The weight factor w is a decreasing exponential function, analogous to the factor introduced by Norrbin to account for stepped banks (Norrbin 1974). The expression of the weight distribution in the ship bound coordinate system is:

$$w = e^{-\left(\xi_y \frac{|y|}{y_{infl}} + \xi_z \frac{|z|}{T}\right)} \qquad (3)$$

The influence distance y_{infl} can be described as the boundary between open and confined water. If the ship-bank distance exceeds this value, no (significant) influence of the bank on the forces and moments on the ship will be observed (Lataire & Vantorre 2008).

The integration of the weight factor over the channel cross section at both sides of the vessel can be calculated with equations (4) and (5). Here the weight factor can be seen as a (ship dependent) overlay sheet which is placed over the cross section under consideration. All 'water particles' are taken into account, also the particles at a distance far away from the vessel but the weight value for these particles will be insignificantly small.

$$\chi_s = \int_0^h \int_0^{y_s} e^{-\left(\xi_y \frac{|y|}{y_{infl}} + \xi_z \frac{|z|}{T}\right)} dy\, dz \qquad (4)$$

$$\chi_p = \int_0^h \int_0^{y_p} e^{-\left(\xi_y \frac{|y|}{y_{infl}} + \xi_z \frac{|z|}{T}\right)} dy\, dz \qquad (5)$$

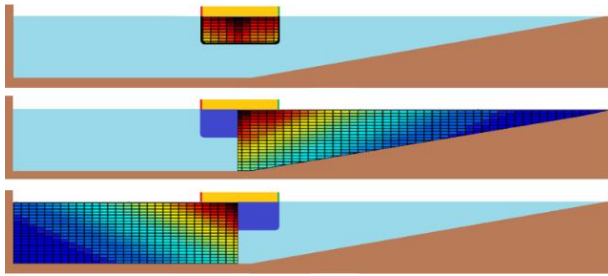A graphical interpretation of χ_p and χ_s is shown in Figure 9.

Figure 9. Graphical interpretation (top down) of χ_{ship}, χ_S (the integrated area at starboard) and χ_P (the integrated and weighted area at port)

The dimensionless distance to bank parameter d2b (or its inverse d2b^{-1}) is by definition:

$$d2b^{-1} = \frac{\chi_{ship}}{2\chi_s} - \frac{\chi_{ship}}{2\chi_p} \qquad (6)$$

The purpose of the introduction of d2b^{-1} is to obtain a parameter to which the forces Y_A and Y_F are proportional:

$$Y_A \propto d2b^{-1} \qquad (7)$$

$$Y_F \propto d2b^{-1} \qquad (8)$$

The values of coefficients ξ_y and ξ_z in equations (4) and (5) have been determined with the regression program "R" (Venables et al. 2002) making use of the model tests results. Both coefficients are constant for each ship – draft combination.

χ_s will be equal to χ_p when sailing on the centre line of a symmetric cross section and as a consequence d2b^{-1} will be zero, which means that the lateral effects of both banks will eliminate each other. When sailing in unrestricted waters the values χ_s and χ_p will be equal and again d2b^{-1} = 0.

The lateral force at the aft perpendicular Y_A of ship model T0Z is plotted in Figure 10. This plot contains results of model tests carried out at a forward speed according to 10 knots full scale, a water depth of 150% of the draft and a constant propeller rate 554 rpm (model scale). In this figure six different bank geometries (3 vertical banks and 3 surface piercing banks) are included, with four different lateral positions.
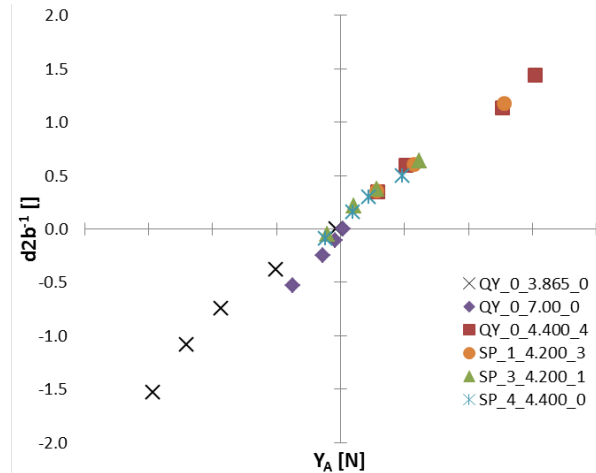

Figure 10. d2b^{-1} vs Y_A for T0Z, 10kts, 554rpm, h=1.50T (the horizontal axis is intentionally left blank for reasons of confidentiality. The origin (0,0) lies on the intersection of both axes).

4.2 BLOCKAGE RATIO

The (classic) definition of the blockage m (equation 9) is known as the fraction of the area a vessel (A_M) occupies in the entire cross section of a fairway (Ω) and is an indication of the squat (running sinkage) and increased resistance in the cross section. However, this ratio is independent of the lateral position of the vessel in the fairway which is a constraint because the (averaged) return flow will be larger for a ship sailing closer to the bank than for a ship sailing more to the centre of the cross section.

$$m = \frac{A_M}{\Omega} \qquad (9)$$

To overcome this constraint, the equivalent blockage m_{eq} is introduced (Lataire et al. 2015a). Similar as d2b this new equivalent blockage m_{eq} should meet some conditions:

- take into account the area of the waterway cross section Ω
- be sensible for the relative position of the ship in the cross section
- be zero when sailing in deep and unrestricted areas
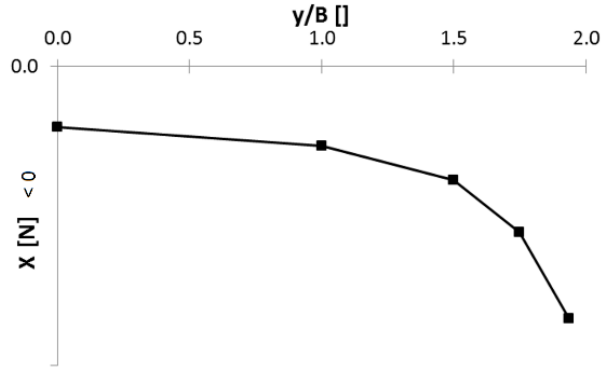- have the unit value one as maximal theoretic value

Figure 11. The longitudinal bank effect X_{BANK} plotted to five lateral positions of the ship model in a rectangular cross section

The equivalent blockage is defined in equation 10 and takes into account the weight distribution w (and the integration result χ) as expressed in previous section.

$$m_{eq} = \frac{1}{2}\left(\frac{\chi_{ship}}{2\chi_s} + \frac{\chi_{ship}}{2\chi_p}\right) - \frac{\chi_{ship}}{\chi_{ocean}} \qquad (10)$$

In Figure 11 the lateral force X_{BANK} is plotted for the ship model T0Z at five different positions (all other input parameters remain the same) in the rectangular cross section with width $W_h = 5$ B and water depth 1.5 T.
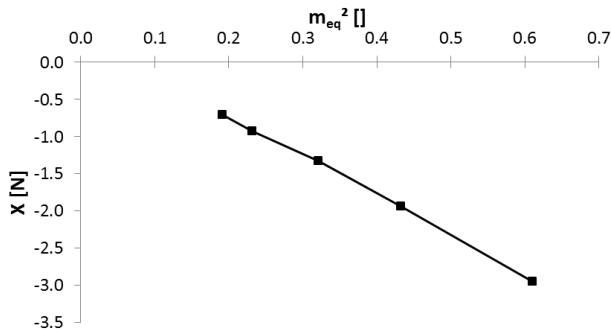
Figure 12. Influence of the lateral position on the longitudinal bank effect X_{BANK} in a rectangular cross section and the relation between X_{BANK} and the square of m_{eq} for the same tests

When the same longitudinal force X_{BANK} is plotted to the square of m_{eq} Figure 12 is obtained; a linear relationship is observed.

5.   TUCK NUMBER

The influence of the forward speed of the vessel, the water depth and characteristics of the propeller action are all integrated in one dimensionless number. In (Tuck 1966) a non-dimensional parameter was introduced, which will be referred to as the Tuck number, (Tu) and is a function of the water depth dependent Froude number Fr_h (equation 2):

$$Tu(V) = \frac{Fr_h{}^2}{\sqrt{|1-Fr_h{}^2|}} \qquad (11)$$

This dimensionless number increases rapidly when the ship sails at a velocity closer to the critical speed (Figure 13) in open (laterally unrestricted, but shallow) water ($= Fr_h = 1$)
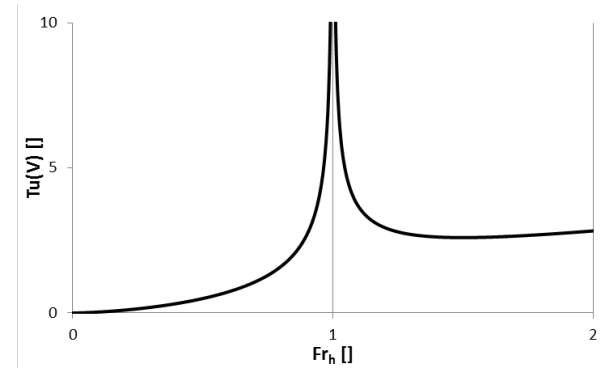

Figure 13. The Tuck number Tu(V) in the sub ($Fr_h<1$) and super critical ($Fr_h>1$) speed region

The critical velocity is the highest velocity at which both a stationary return flow and sinkage of the free water surface and the ship are possible (subcritical speed range). At higher speeds, the ship enters the transcritical speed region, in which no stationary equilibrium exists. At even higher speeds, a stationary state is reached again in the supercritical speed range, which is characterised by an elevation of the free surface and a reduced return flow (Balanin 1977).

The critical velocity decreases in confined (i.e. laterally restricted) waters and the critical Froude number Fr_{crit} will be smaller than 1. In (Schijf 1949) the critical Froude number is calculated taking into account the blockage m:

$$Fr_{crit} = \left(2\, sin\left(\frac{Arcsin(1-m)}{3}\right)\right)^{\frac{3}{2}} \qquad (12)$$

The Tuck number is now adapted to Tu_m causing a shift to the left of the vertical asymptote in Figure 13, which is now located at the critical Froude number Fr_{crit}:

$$Tu_m(V) = \frac{\left(\frac{Fr_h}{Fr_{crit}}\right)^2}{\sqrt{1-\left(\frac{Fr_h}{Fr_{crit}}\right)^2}} \qquad (13)$$

The flow around the hull is not only determined by the forward speed, but also by the propeller action. A propeller generating (positive) thrust, at a positive rotational speed, accelerates the water flow passing the propeller disk and therefore increases the velocity of the water between bank and ship. The influence of the propeller action on the lateral force will be modelled as a partial increase of the forward speed of the vessel (V_{eq}):

$$V_{eq} = V + \xi_{VT} V_T \qquad (14)$$

The coefficient ξ_{VT} takes a value between 0 and 1 and the thrust velocity V_T is calculated based upon the thrust T_P (as measured on the propeller shaft).

$$V_T = sign(T_P) \sqrt{\frac{|T_P|}{\frac{1}{2}\rho\pi\frac{D^2}{4}}} \qquad (15)$$

Figure 14 illustrates that the new parameter $Tu_m(V_{eq})$ is indeed suitable for modelling the lateral forces fore and aft. A wide range of water depths, ship speeds and propeller actions are included.

$$Y_A \propto Tu_m(V_{eq}) \qquad (16)$$
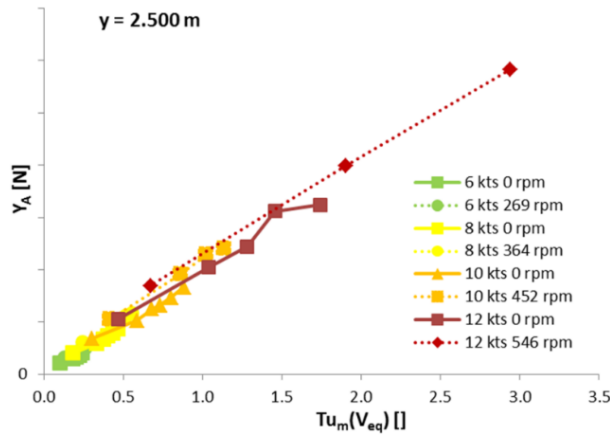
$$Y_F \propto Tu_m(V_{eq}) \qquad (17)$$

Figure 14. Y_A plotted to $Tu_m(V_{eq})$ for all the model tests with A01 in cross section QY_0_7.00_0 at a lateral position y = 2.500 (ordinate is intentionally left blank for reasons of confidentiality)

Similar as for the lateral forces at the fore and aft perpendiculars, the longitudinal bank effect force X_{BANK} appears to be proportional to the Tuck number $Tu_m(V_{eq})$.

$$X_{BANK} \propto Tu_m(V_{eq}) \qquad (18)$$

In Figure 15 the correlation between the adapted Tuck number Tum and the longitudinal force X_{BANK} is visualised and the value meq is added as a label to the data points. The relation between the Tuck number and X_{BANK} cannot be visualised exactly because the blockage m_{eq} is not exactly the same for the ten tests plotted. As a consequence, the impact of m_{eq} is not excluded entirely in Figure 15 to support the relation 20.
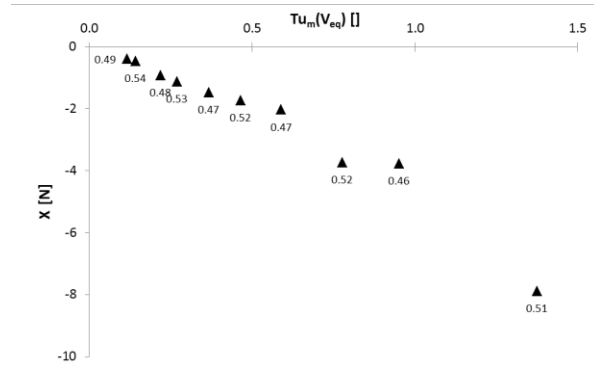

Figure 15. Relation between adapted Tuck number Tu_m and the longitudinal force for a variation of m_{eq} from 0.46 up to 0.54 (added as label to the data points)

6. MATHEMATICAL MODEL

The combination of equation (7) and equation (16) results in:

$$Y_A = \xi_\rho \, \Delta \, d2b^{-1} \, Tu_m(V_{eq}) \qquad (19)$$

Remark that the displacement force Δ [N] is the only dimensional number on the right hand side of the equation. To get an equation instead of a proportion the constant ξ_ρ is added. Only four coefficients (ξ_ρ, ξ_y and ξ_z in d2b and $\xi_{VT,A}$) are used in the mathematical model for Y_A. These four coefficients are valid for one displacement condition of one ship.

The lateral force at the forward perpendicular induced by bank effects is modelled as:

$$Y_F = \xi_\rho \, \Delta \, d2b^{-1} \, Tu_m(V_{eq}) \, f(h, T, Fr, \xi_{hT} \, \xi_h) \qquad (20)$$

This formulation consists of six independent coefficients (ξ_ρ ξ_y ξ_z $\xi_{VT,F}$ ξ_{hT} ξ_h). In very deep water there is always attraction towards the closest bank while in very shallow water a repulsion force away from the closest bank is consistent. In between, the force can have both directions and therefore a relative water depth and Froude number dependent function (Figure 16) is introduced f(h,T,Fr,ξ_{hT} ξ_h). A positive value indicates an attraction force, a negative value a repulsion away from the closest bank.

The lateral force Y_A is for all water depths an attraction force directed towards the closest bank. The attraction force at the aft perpendicular Y_A is, in deeper water, larger than the attraction force at the forward perpendicular Y_F. The combination of these two forces results in an overall attraction towards the closest bank in combination with a bow out moment. In very shallow water the magnitude of the repulsion force at the forward perpendicular can be larger than the attraction force at the aft perpendicular. Both forces will then result in an overall repulsion force away from the closest bank but still in combination with a (large) bow away moment.
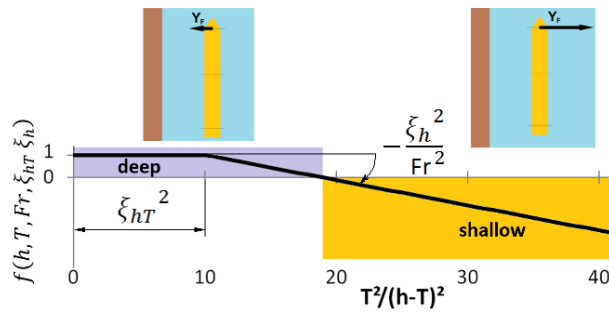
Figure 16 the function $f(h, T, Fr, \xi_{hT} \xi_h)$ which results in an attraction force or repulsion force Y_F

The product of the square of the equivalent blockage m_{eq} and the adapted Tuck number Tu_m are proportional to the longitudinal bank force X_{BANK}. Multiplied with the displacement force Δ to introduce a force dimension and with the ship dependent coefficient ξ_X to cope with the proportionality, the formula for X_{BANK} becomes:

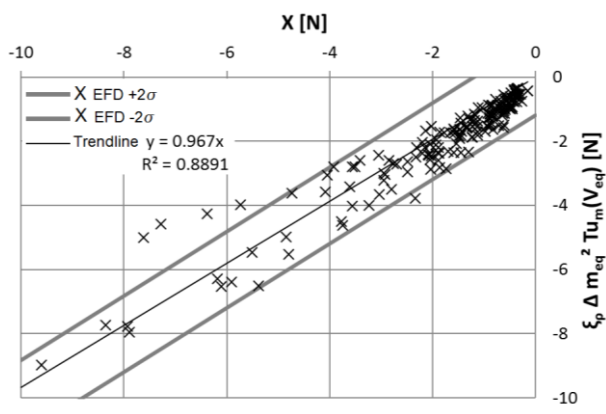$$X_{BANK} = \xi_X \Delta \, m_{eq}^2 \, Tu_m(V_{eq}) \qquad (21)$$

Figure 17 the model for X_{BANK} plotted to the force X_{BANK} derived from model tests with the kvlcc2 ship model

The longitudinal force X (assumed to be equal to X_{BANK}) for all model tests with a VLCC ship model at a propeller rate according to self-propulsion in open water are plotted in Figure 17 (171 model tests). The relation between the modelled force and the force derived from model tests is satisfying although some deviation is observed. This deviation is ascribed to the error introduced in extracting the force X_{BANK} from the measured (longitudinal) forces during the model tests. The mathematical model for X_{BANK} runs on only one dedicated coefficient ξ_X (the other coefficients are copied from the mathematical model for the lateral force Y_A.) and is a very robust mathematical model.

7. QUANTITATIVE EXAMPLES

A quantitative comparison between different sloped banks is given in Table 5. The forces and moments are given for a (fictive) container carrier of 350 m long, 50 m wide and with an initial draft of 12.5 m. All four cross

sections of the fairway have the same width W_h of 500 m (or 10 B) at the full water depth (=15 m). The banks at port and starboard have the same slope and the ship sails at 8 knots at a distance between the toe of the starboard bank and her own starboard side of 50 m (= B). The bank effects are calculated for 4 different sloped banks;

- vertical quay wall (1/0)
- steep sloped bank of 45° (1/1)
- bank with slope 1/3
- gentle sloped bank of 1/8 (about the underwater angle of repose of sand)

Table 5. Bank forces and moment induced on container carrier

slope	X_{BANK}	Y_{BANK}	N_{BANK}	δ/δ_{max}	β
-	*ton*	*ton*	*ton m*	*%*	*°*
1/0	-32	94	-19110	78	0.39
1/1	-24	78	-15716	64	0.32
1/3	-15	56	-11291	46	0.23
1/8	-7	30	-6061	25	0.12

The increased resistance (negative value for X_{BANK} means resistance) on the vessel when sailing along the vertical wall is twice as large as sailing along the bank with slope 1/3 and four times as large when sailing along the most gentle sloped bank of 1/8. Bear in mind that the overall cross section area of the 1/8 sloped bank is also 24% larger than the vertical banks (because W_h is the same for all four cross sections in this example).

Bear in mind that an increased resistance in confined and restricted waters may cause an increased fuel consumption, but has no adverse effect on the ship's controllability because the propeller load will increase, which will have a beneficial effect on the rudder induced forces.

The overall lateral bank force Y_{BANK} is in present example always an attraction force (directed towards the closest bank). This is the reason why bank effects are also known as bank suction but in very shallow water this attraction force becomes an overall repulsion force, hence the better use of the term bank effects. The attraction force is along the vertical bank about three times as large as along the beachy bank of 1/8.

The yaw moment is always (at all water depths) a bow away moment and its magnitude about the double when sailing along the 1/3 bank compared to the 1/8 bank and more than three times larger for the vertical bank compared to the 1/8 bank.

Both the lateral force Y_{BANK} and the yaw moment N_{BANK} can be compensated by a combination of drift angle (β) and amount of helm (δ). In Table 5 this equilibrium is

calculated for a propeller rate of 80% of telegraph position harbour full.

This means that the ship sails at an equilibrium between the bank effects (Y_{BANK} and N_{BANK}) and the drift and rudder forces when sailing at a drift angle of 0.32° (bow towards the bank) and an amount of rudder of 64% (to port) of the full rudder deflection (35°) when sailing along the 45° sloped bank under the previous conditions. In this example a significant amount of the rudder capacity is thus required to compensate the bank effects.

8. CONCLUSIONS

The data set on bank effects consists of more than 8 000 unique model test setups (which is by far the most systematic and elaborate research ever carried out on this subject). Eleven different ship models (both inland and seagoing) have been tested at a broad range of draft to water depth ratios. The captive towing tests were conducted at a range of forward speeds and propeller actions along a wide range of different bank geometries at different lateral positions of the ship from the bank. During the model tests the horizontal forces and moments on the hull, propeller(s) and rudder(s), as well as the vertical ship motions (squat) were measured. These measurements are the input for the analysis of bank effects and the creation of a new mathematical model which is – thanks to its simplicity of formulation and robustness – a contribution to more reliable simulations when navigating close to the margins. The three modelled forces are:

- The increased resistance (longitudinal force) X_{BANK}
- The lateral force at the forward perpendicular Y_F (attraction force in deep water, repulsion force in shallow water, Figure 18)
- The lateral force at the aft perpendicular Y_A (always an attraction force)
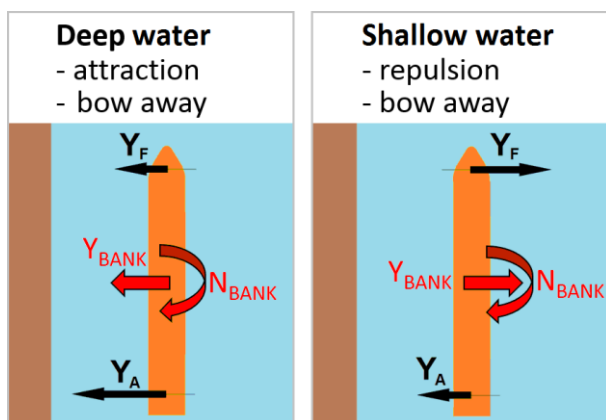

Figure 18 summary of the bank effect induced lateral forces and yaw moment in deep and shallow water

It is trivial that both lateral forces Y_F and Y_A can easily be decomposed in an overall lateral force Y_{BANK} and overall yaw moment N_{BANK} as is done by other authors writing about bank effects.

9. ACKNOWLEDGEMENT

10. REFERENCES

1. BALANIN, V., 1977. *Peculiarities of navigation on canals and restricted channels, originating hydraulic phenomena associated with them and their effect on the canal bed*. In 24th International Navigation Congress. Leningrad.
2. DELEFORTRIE, G., GEERTS, S. & VANTORRE, M., 2016. *Towing tank for manoeuvres in shallow water*. In MASHCON 4.
3. LATAIRE, E. & VANTORRE, M., 2008. *Ship-Bank Interaction Induced by Irregular Bank Geometries*. In 27th Symposium on Naval Hydrodynamics. Seoul, Korea, pp. 5–10.
4. LATAIRE, E., VANTORRE, M. & DELEFORTRIE, G., 2015a. *Longitudinally Directed Bank Effects*. In MARSIM 2015. Newcastle.
5. LATAIRE, E., VANTORRE, M. & DELEFORTRIE, G., 2015b. *The influence of the ship's speed and distance to an arbitrarily shaped bank on bank effects* (presentatie). In 34th International Conference on Ocean, Offshore and Arctic Engineering (OMAE). St. John's, Newfoundland, Canada.
6. LATAIRE, E., VANTORRE, M. & ELOOT, K., 2009. *Systematic Model Tests on Ship-Bank Interaction Effects*, Ghent University.
7. NORRBIN, N.H., 1974. *Bank Effects on a Ship Moving through a Short Dredged Channel*. In R. D. Cooper & S. W. Doroff, eds. *10th ONR*. Office of Naval Research, pp. 71–88.
8. PAPANIKOLAOU, A. ET AL., 2015. *Energy Efficient Safe Ship Operation*. In Influence of EEDI on Ship Design. London.
9. SCHIJF, J.B., 1949. *Protection of Embankments and Bed in Inland and Maritime Waters, and in Overflow or Weirs*. In XVII International Navigation Congress, Lisbon, Section I. pp. 61–78.
10. STERN, F. & AGDRUP, K., 2008. SIMMAN 2008 Workshop on Verification and Validation of Ship Maneuvering Simulation Methods. In *Workshop*

Proceedings. p. 2008. Available at: http://scholar.google.com/scholar?hl=en&btnG=Se arch&q=intitle:Workshop+on+Verification+and+V alidation+of+Ship+Manoeuvring+Simulation+Met hods#1 [Accessed June 13, 2014].

11. TUCK, E.O., 1966. *Shallow-water flows past slender bodies*. Journal of Fluid Mechanics, 26, pp.81–95.

12. VENABLES, W., SMITH, D. & TEAM, R.D.C., 2002. *An introduction to R*, Available at: http://www.math.vu.nl/sto/onderwijs/statlearn/R-Binder.pdf [Accessed May 23, 2014].

13. ZOU, L. & LARSSON, L., 2013. *Computational Fluid Dynamics (CFD) Prediction of Bank Effects Including Verification and Validation*. Journal of Marine Science and Technology, 18, pp.310–323. Available at: http://link.springer.com/article/10.1007/s00773-012-0209-7 [Accessed November 29, 2013].